On the Role of Water in Peroxidase Catalysis: A Theoretical Investigation of HRP Compound I Formation

Pietro Vidossich,[†,‡,#] Giacomo Fiorin,[§] Mercedes Alfonso-Prieto,[†,‡] Etienne Derat,[⊥] Sason Shaik,*[,¶] and Carme Rovira*[,†,‡,∥]

Laboratori de Simulació Computacional i Modelització(CoSMoLAB), Parc Científic de Barcelona, Josep Samitier 1-5, 08028 Barcelona, Spain, Institut de Química Teòrica i Computacional (IQTCUB), Barcelona, Spain, Center for Molecular Modeling, University of Pennsylvania, 231 South 34th Street, Philadelphia, Pennsylvania 19104-6323, Institut Parisien de Chimie Moléculaire, UMR 7201-CNRS, Université Pierre et Marie Curie, 4 place Jussieu C. 229, 75505 Paris, France, Institute of Chemistry and the Lise Meitner-Minerva Center for Computational Quantum Chemistry, The Hebrew University of Jerusalem, Givat Ram Campus, 91904 Jerusalem, Israel, and Institució Catalana de Recerca i Estudis Avançats (ICREA), Passeig Lluís Companys, 23, 08018 Barcelona, Spain

Received: November 27, 2009; Revised Manuscript Received: March 5, 2010

We have investigated the dynamics of water molecules in the distal pocket of horseradish peroxidase to elucidate the role that they may play in the formation of the principal active species of the enzymatic cycle (compound I, $Por^{\circ+}-Fe^{IV}=O$) upon reaction of the resting Fe^{III} state with hydrogen peroxide. The equilibrium molecular dynamics simulations show that, in accord with experimental evidence, the active site access channel is hydrated with an average of two to three water molecules within 5 Å from the bound hydrogen peroxide. Although the channel is always hydrated, the specific conformations in which a water molecule bridges H_2O_2 and the distal histidine, which were found (Derat; et al. *J. Am. Chem. Soc.* **2007**, *129*, 6346.) to display a low-energy barrier for the initial acid−base step of the reaction, occur with low probability but are relevant within the time scale of catalysis. Metadynamics simulations, which were used to reconstruct the free-energy landscape of water motion in the access channel, revealed that preferred interaction sites within the channel are separated by small energy barriers (<1.5 kcal/mol). Most importantly, water-bridged conformations lie on a shoulder just 1 kcal/mol above one local minimum and thus are easily accessible. Such an energy landscape appears as a requisite for the effectiveness of compound I formation, whereby the H-bonding pattern involving reactants and catalytic residues (including the intervening water molecule) has to rearrange to deliver the proton to the distal OH moiety of the hydrogen peroxide and thereby lead to heterolytic O−O cleavage. Our study provides an example of a system for which the "reactive configurations" (i.e., structures characterized by a low barrier for the chemical transformation) correspond to a minor population of the system and show how equilibrium molecular dynamics and free-energy calculations may conveniently be used to ascertain that such reactive conformations are indeed accessible to the system. Once again, the MD and QM/MM combination shows that a single water molecule acts as a biocatalyst in the cycle of HRP.

1. Introduction

Heme enzymes constitute an important group of enzymes that are present in almost all aerobically respiring organisms.[1] They perform a broad range of protein-specific reactions such as oxidation, oxygenation, hydroxylation, and chlorination.[1,2] Their reactivity is determined by the protein matrix in which the heme prosthetic group is buried, and therefore, unraveling the details of such effective modulation has become an active field of research.[3] Because the active sites of these families of enzymes are generally accessible to solvent molecules,[4−6] it is entirely possible that water molecules could play a role in catalysis, as postulated by several authors.[7−10]

An important class of heme enzymes are heme peroxidases, which oxidize a variety of substrates by reacting first with hydrogen peroxide. Horseradish peroxidase (HRP) is among the most studied peroxidase enzymes.[1,2] The main function of HRP appears to be the oxidation of phenols which subsequently polymerize and serve to build and repair the cell walls in higher plants.[1] The catalytic mechanism of HRP, as well as of other heme enzymes (peroxidases, catalases, and cytochromes P450s), starts with the reaction of the resting ferric (Fe^{III}) state with a molecule of hydrogen peroxide, H_2O_2, (although, in vitro, other oxidants may be used, e.g., alkyl and aryl peroxides)[2] to form a high-valent iron−oxo intermediate named compound I (Cpd I). During this process, the heme is oxidized to an oxoferryl porphyrin π-cation radical species ($Por^{\circ+}-Fe^{IV}=O$), as shown in reaction 1 for, for example, HRP. In some cases, such as in cytochrome C peroxidase (CCP),[3] the cation radical resides on a protein residue.

* To whom correspondence should be addressed. E-mail: crovira@pcb.ub.es (C.R.); sason@yfaat.ch.huji.ac.il (S.S.).
† Parc Científic de Barcelona.
‡ Institut de Química Teòrica i Computacional (IQTCUB).
§ University of Pennsylvania.
⊥ Université Pierre et Marie Curie.
¶ The Hebrew University of Jerusalem.
∥ Institució Catalana de Recerca i Estudis Avançats (ICREA).
Present address: Unitat de Química Física, Universitat Autònoma de Barcelona, 08193 Bellaterra. Spain.

10.1021/jp911170b
Published on Web 03/29/2010

$$\text{Enz(Por}-\text{Fe}^{\text{III}}) + \text{H}_2\text{O}_2 \rightarrow \text{Cpd I(Por}^{\bullet+}-\text{Fe}^{\text{IV}}=\text{O}) + \text{H}_2\text{O} \quad (1)$$

As inferred from kinetics studies, the formation of Cpd I in HRP follows a stepwise mechanism, passing through the formation of at least one reversible intermediate.[11−13] Much effort has been dedicated to finding the conditions which stabilize the putative intermediates and thus enable its characterization.[2,14] Early kinetics studies showed that Cpd I formation is not diffusion-limited,[15] and therefore, formation of the ferric peroxide complex [Enz(Por−Fe$^{\text{III}}$)−H_2O_2] does not determine the rate of the process. This complex is expected to evolve by deprotonation from one OH group of H_2O_2 and reprotonation of the other one, thus leading to the liberation of the water molecule in reaction 1. A mechanistic pathway was proposed earlier by Poulos and Kraut based on the analysis of the X-ray structure of cytochrome c peroxidase (CCP)[16,17] (Figure 1a). In this pathway, the histidine residue on the distal side of the heme (His42) deprotonates H_2O_2, leading to the formation of a ferric hydroperoxide intermediate (Por−Fe$^{\text{III}}$−OOH) that was later called compound 0 (Cpd 0). This intermediate evolves to Cpd I, forming one coproduct water molecule. Mutagenetic studies[18−20] supported the Poulos−Kraut mechanism showing that peroxidase mutants lacking the distal side His display a reduced rate of Cpd I formation.

Even though neither the enzyme−H_2O_2 complex nor Cpd 0 of HRP have yet been experimentally characterized for HRP, X-ray structures of the ferric−hydroperoxo and ferric−peroxo forms have been determined for chloroperoxidase[21] and myoglobin.[22] Thus, it is believed that HRP also functions via Cpd 0, although a detailed microscopic view of Cpd I formation in HRP is still lacking. In particular, it is yet unclear whether the rate-limiting step of the reaction consists of the formation of Cpd 0 or rather its evolution to Cpd I as different experiments resulted in different interpretations.[18,23,24]

Interestingly, Watanabe and co-workers found that the rate of HRP Cpd I formation in an organic solvent increases with water concentration,[13] suggesting that water might play a role in the reaction. Later on, Jones et al.[7] introduced the concepts of wet/dry Cpds 0 and I to differentiate the reactivity of Cpd I in peroxidases (active site water-exposed) and catalases (active site buried into the protein), respectively. It was also suggested that an active-site water molecule might relay a proton-transfer event in peroxidases.[7] Most HRP X-ray structures reveal an array of water molecules in the active site for all of the species that were solved.[4] Particularly interesting is the structure of the oxyferrous complex Por−Fe$^{\text{II}}$−OO (also known as Cpd III), which is the closest model for the ferric−peroxide complex,[25] and which contains two water molecules in the distal pocket,[4] one of them interacting directly with dioxygen.

On the basis of the above considerations, we recently explored a reaction pathway for Cpd I formation in which a single water molecule bridges the long distance between His42 and the proximal proton of H_2O_2[8] and thereby dramatically reduces the barrier of Cpd 0 formation in HRP (i.e., deprotonation of H_2O_2; see Figure 1b) from ∼20 to ∼5 kcal/mol.[8,26] Thus, this water molecule is not merely a spectator in the reaction but a catalytic entity, as found in theoretical studies of other enzymatic reactions (see, e.g., refs 9, 27−29). Following H_2O_2 deprotonation (Figure 1b), a change in the active-site H-bonding pattern and the leak of the catalytic water molecule allows for the transfer of the proton from the distal histidine to the distal peroxide oxygen and the concomitant cleavage of the peroxide OO bond, leading to Cpd I (Figure 1b). The two pathways ("dry" and "wet") pass through the same intermediates (those proposed

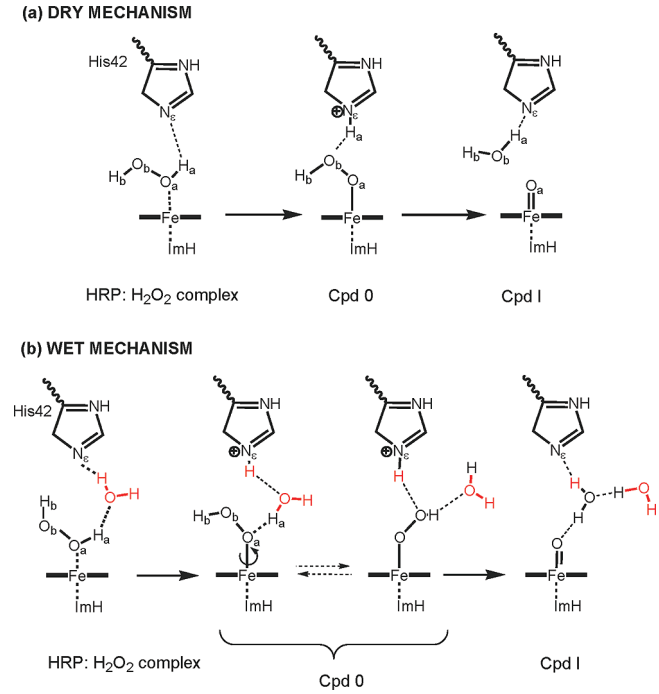

Figure 1. (a) The original Poulos−Kraut mechanism of peroxidase compound I formation[17] (referred as dry mechanism in the text). (b) The same mechanism with the involvement of a water molecule (wet mechanism), as proposed in our previous work.[8] The initial HRP−H_2O_2 configuration is named the reactive conformation in the text.

by Poulos and Kraut[17]) but differ in that the distal histidine in the wet mechanism, although still acting as a general base, does not directly abstract the proximal proton from the peroxide. Recently, a molecular dynamics (MD) study[30,31] on HRP did not find water molecules in the vicinity of hydrogen peroxide, a result that, though unsupported by the above-cited experimental evidence, still questions the validity of the wet mechanism, which was supported by our MD studies.

The present study, based on classical MD simulations, complements our previous work investigating the conformational space of the bound peroxide and the dynamics of water molecules in the heme distal pocket. Thus, we apply here the metadynamics (MetD) approach[32] to properly sample the free-energy surface of the water translocation along the heme access channel. It will be shown that H_a from the peroxide (see Figure 1a for atom labels) is H-bonded to a water molecule that easily bridges the peroxide and His42, right in place to facilitate formation of Cpd 0. Conformations in which distal His is directly hydrogen-bonded to the peroxide (dry configurations) are also found, but with lower probability than the wet configurations. Therefore, the one-water wet mechanism emerges as the one that satisfies the conditions of (i) involving a likely configuration and (ii) having a low deprotonation energy barrier toward Cpd 0. Finally, we propose a reaction mechanism for the Cpd I formation that agrees with the available experimental information.

2. Computational Details

2.1. Model System. Calculations were based on the HRP−H_2O_2 complex previously reported.[8,26] The model is based on the X-ray structure of HRP Cpd I (PDB code: 1HCH).[4] A complete model of the solvated enzyme was built by modifying the active site to include H_2O_2 and by adding the missing hydrogen atoms according to standard geometries. All aspartates and glutamates were considered as negatively charged, and

arginines and lysines were considered as positively charged. Histidines (His40, 42, 170) were singly protonated, His170 and the distal side His42 at N_δ and His40 at N_ε. Calcium ions, observed in the X-ray structure,[4] were retained in the model. The complex was solvated with 20512 water molecules and two Cl^- ions were included in the model to neutralize the simulation cell.

2.2. Force Field Parameters. Classical MD studies have been performed before on HRP and CCP to investigate the mode of binding of peroxide and its interactions with active-site residues.[33−35] Compared with these previous studies,[33−35] in which the iron−peroxide was treated as nonbonded, here, we have focused on the iron-bound peroxide to characterize its conformational freedom and interactions with active-site water molecules.

The AMBER (version 99)[36−38] and TIP3P[38] force fields were used for the protein and for water, respectively. Bonding and van der Waals parameters for the porphyrin were taken from the AMBER distribution. The derivation of force field parameters for the Fe−H_2O_2 fragment was based on a gas-phase ab initio molecular dynamics (CPMD) simulation (see below for computational details) of the iron(III) porphyrin−H_2O_2 complex (unsubstituted porphyrin). The structure of H_2O_2 turned out to be very similar to the one described by the GAFF force field.[39] Therefore, we adopted the GAFF parameters to describe the internal H_2O_2 interactions. Harmonic bond and angle parameters that involve the Fe and O_a atoms were obtained from the distribution of geometries observed in the CPMD simulation (force field parameters are given in the Supporting Information, SI). A single dihedral transition was observed during the CPMD simulation, not sufficient for the derivation of torsional parameters. Thus, CPMD geometry optimizations for different values of the N_β−Fe−O_a−H_a dihedral (Ω) were performed. The energy profile (at 30° intervals) was fitted by a function of the form $V[1 + \cos(\Omega - \text{phase})]$. Charges were developed according to the RESP methodology.[40] Four conformations of the heme−H_2O_2 complex were extracted from a QM/MM CPMD simulation (see SI for computational details), and the electrostatic potential on a grid at the water-accessible surface was calculated at the HF/6-31G* level of theory (for consistency with the AMBER force field) for each conformer. In the RESP fitting, point charges on the porphyrin atoms were fixed at the AMBER heme−Fe^{II} values, and only the charges on the iron, the four pyrrol nitrogens, and H_2O_2 were allowed to vary. All derived parameters are reported in the SI, and a comparison of geometrical parameters from ab initio and force-field-based molecular dynamics is given in Table S1 (SI).

2.3. Gas-Phase CPMD. To derive parameters for the iron−H_2O_2 interactions, gas-phase ab initio molecular dynamics simulations[41] were performed for an iron(III) porphyrin−H_2O_2 model (no substituents on the porphyrin). Calculations were based on spin-dependent density functional theory (DFT-LSD).[42,43] The study was limited to the doublet state, which is one of the two lowest states of the enzyme−H_2O_2 complex (the doublet state is almost degenerate with the quartet state) and becomes the ground state of Cpd 0.[26] Valence orbitals were expanded with a plane wave basis set (up to 70 Ry), and Martins−Troullier pseudopotentials[44] were used to describe the core−valence shell electrons interactions. The Becke[45] and Perdew[46] functionals were used for exchange and correlation interactions, respectively. The system was placed in a supercell and treated as isolated.[47] After 0.5 ps of equilibration, 2 ps CPMD simulations were performed at 300 K, coupling the systems to a Nosé−Hoover thermostat,[48,49] using a time step of 5 au and a fictitious electron mass of 800 au to solve the equations of motion.

2.4. Classical MD. Calculations were performed with the NAMD program.[50] Periodic boundary conditions were applied with a cubic simulation cell of ∼87 Å per edge. Long-range electrostatic interactions were treated with the PME method.[38] A 12 Å cutoff for the real part of the electrostatic and for van der Waals interactions was used. The integration time step was 1 fs. After 1 ns of solvent equilibration and energy minimization of the whole system, the model was slowly heated up to 300 K in 1.9 ns. Then, 4 ns equilibrium MD simulations were performed at constant temperature (300 K) and pressure (1 atm).

The trajectory from the MD simulation (conformations were stored every 1 ps) was analyzed in search of the conformation in which a water molecule bridges the peroxide and His42, called the reactive conformation in the text. For its definition, the following parameters were chosen: $H_a\cdots O^W < 2.5$ Å, $N_\varepsilon\cdots O^W < 3$ Å, and angle $N_\varepsilon\cdots O^W\cdots H_{1,2}{}^W > 120°$.

2.5. Metadynamics Simulations. Metadynamics[32] (MetD) was used to improve the sampling of conformational space and to reconstruct the free-energy surface (FES) for the following two processes: the rotation of the peroxide around the Fe−O_a bond (MetD-1 hereafter) and the approach of a water molecule to the hydrogen peroxide and the distal histidine (MetD-2 hereafter). In MetD-1, we computed the FES as a function of one collective variable, the dihedral defined by the N_β−Fe−O_a−H_a atoms (see Figure 1 for atom names). In MetD-2, we defined instead two collective variables to monitor the formation of the H-bonds between a water molecule and the peroxide or the distal His (His42); the closest water molecule to the peroxide at the beginning of the metadynamics was chosen. The collective variables used were the distance between H_a and O^w (CV_1) and the coordination number[51] between N_ε and $H_1{}^w$ or $H_2{}^w$ (CV_2).

$$CV_2(N_\varepsilon;H_1^w,H_2^w) = \frac{1-(|r(N_\varepsilon)-r(H_1^w)|/d)^n}{1-(|r(N_\varepsilon)-r(H_1^w)|/d)^m} + \frac{1-(|rN_\varepsilon)-r(H_2^w)|/d)^n}{1-(|r(N_\varepsilon)-r(H_2^w)|/d)^m}$$

with the following parameters: $d = 2.5$ Å, $n = 6$, $m = 12$. CV_2 quantifies the formation of a hydrogen bond between N_ε and any of the water hydrogens ($H_1{}^w$ or $H_2{}^w$).

Both metadynamics runs were initialized from the last snapshot of the equilibrium MD and were performed using the collective variables module implemented in NAMD 2.7. The reconstruction of the two FESs was performed by inserting Gaussian biasing potentials every 2000 MD steps. The height and width of the Gaussian potentials was set as height = 0.01 kcal/mol, width = 15° (MetD-1), 0.6 Å (MetD-2, CV_1), and 0.3 (MetD-2, CV_2). MetD-1 was considered converged after five recrossings of the initial configuration (4.5 ns of simulated time; see Figure S5, SI), whereas for MetD-2, the reconstruction of the free-energy surface converged after four recrossing events, corresponding to 5.5 ns (see Figures S6, S7, and S8, SI). Gaussian functions applied to the dihedral in MetD-1 were computed by taking into account its 360° periodicity.

2.6. Quantum Mechanics/Molecular Mechanics (QM/MM) Calculations. Starting from the **B3** conformation (see later Figures 4 and 5) found by the MetD-2 simulation, we ran QM/MM calculations with Chemshell[52] in order to compute barriers in the pathway to compound I. To perform the QM/MM

calculations, Chemshell integrates the TURBOMOLE[53] package for QM and the DL-POLY[54] program for MM. The QM/MM calculations involved a QM region comprising the heme, H_2O_2, models of Arg38 and His42, and two solvent water molecules. This active center was described by DFT in the unrestricted Kohn−Sham formalism, employing the B3LYP functional.[55−57] Geometry optimizations were performed with a double-ζ basis set (LACVP[58,59]), and single-point energy corrections were performed with a triple-ζ basis set (TZVP[60]). The rest of the system was treated by classical molecular dynamics, using a force field calibrated for proteins (namely, CHARMM22[61]). The QM/MM geometry optimization included the following residues: Arg_{31}, Ser_{35}, Arg_{38}, Phe_{41}, His_{42}, Phe_{68}, Gly_{69}, Asn_{70}, Ser_{73}, Leu_{138}, Pro_{139}, Ala_{140}, Pro_{141}, Phe_{142}, Ser_{167}, His_{170} (including the heme), Gln_{176}, Phe_{179}, Ile_{244}, Asp_{247}, Phe_{221}, Tyr_{233}, and some selected water molecules close to these residues. Except for the basis set size (TZVP in this study and TZV in our previous work), this is the same computational setup that was used in our previous work to compute the energy barrier for Cpd I formation from the reactive conformation of HRP.[8] To allow comparisons, we recomputed the energy barrier for this conformation using the TZVP basis set.

3. Results

3.1. Equilibrium Molecular Dynamics Simulation. As a first step in our investigation, we performed six nanoseconds of classical MD simulation of the HRP−H_2O_2 complex, using the parameters derived from an ab initio MD simulation (section 2.2) to describe the iron−peroxide interaction. The overall protein structure turned out to be well-maintained during the simulation. The root-mean-square displacement (rmsd) of the protein backbone with respect to the crystal structure reached equilibrium within the first 2 ns (the long equilibration period is due to the slow heating procedure employed), and it remained at ~1 Å for the rest of the simulations (see Figure S1, SI). After equilibration, backbone fluctuations fairly agreed with the experimental pattern.

Analysis of the dynamics of the distal pocket residues revealed that His42 and Arg38 interact with the H_2O_2 molecule most of the time (Figures S2 and S3bc, SI), forming $H_b\cdots N_\varepsilon$ (His42) and $O_b\cdots H$(Arg38) hydrogen bond interactions (only for very short intervals, <0.5 ns, the $H_b\cdots N_\varepsilon$ hydrogen bond breaks). The H_2O_2 molecule is not fixed in space but rotates around the Fe−O_a bond, displaying three preferred orientations (at values $\Omega = -77 \pm 27$, -1 ± 12, and $85 \pm 12°$).

Since we are interested in conformations that could trigger catalysis, we analyzed in detail the MD trajectory in search for snapshots in which either H_a approaches the N_ε of His42 (putative starting conformation for the dry mechanism; see Figure 1a) or a water molecule bridges H_a with His42 (wet mechanism; Figure 1b). During the simulation, the distance between H_a and N_ε of His42 oscillates around an average value of 3.69 Å (Figure S3, SI), a distance clearly too large for proton transfer via the dry mechanism (Figure 1a), which, as we recall, also yields a very large QM/MM barrier of 21.5 kcal/mol. $H_a\cdots N_\varepsilon$ distances shorter than 3 Å were hardly found (0.015% of the analyzed frames), and they typically occurred together with strained hydrogen bonds, that is $\angle O_a{-}H_a{-}N_\varepsilon \approx 90°$). Only two configurations with a nonstrained $H_a\cdots N_\varepsilon$ hydrogen bond were found (Figure S4, SI) during the entire simulation. However, the resulting $H_a\cdots N_\varepsilon$ distances (2.76 and 2.81 Å, respectively) are still rather long for effective proton transfer.

Figure 2a shows the number of water molecules approaching the hydrogen peroxide molecule along the simulation. There

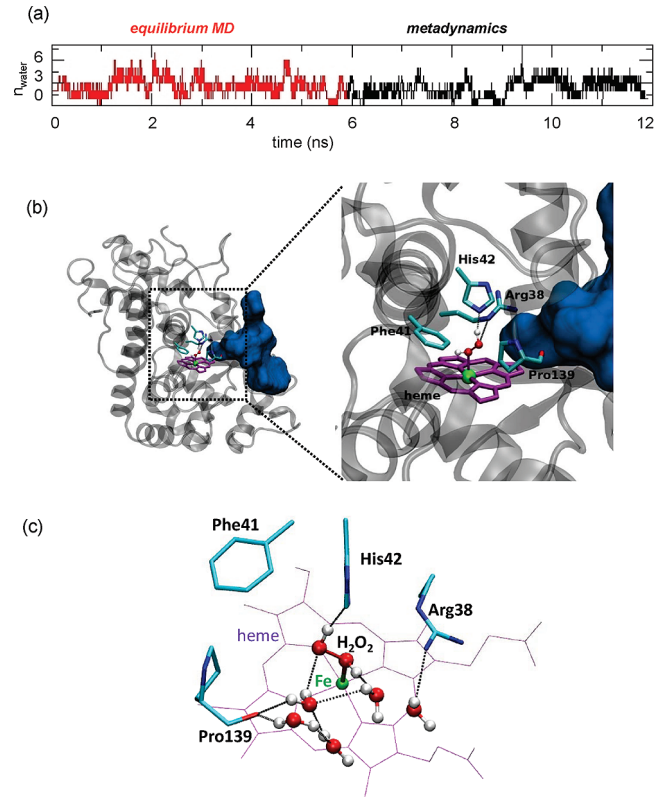

Figure 2. (a) Number of water molecules within 5 Å of hydrogen peroxide obtained in the simulations. (b) Volume of the active site access channel in HRP. (c) Representative hydrated configuration from the equilibrium MD simulation.

are on average 2.6 ± 1.1 water molecules within 5 Å from H_2O_2. This is not unexpected given the sizable channel connecting the active site of HRP with the protein surface (Figure 2b). Most of the time (62% of the analyzed frames), there is at least one water molecule at hydrogen bonding distance from the peroxide. These configurations will be hereafter referred to as "hydrated configurations" (see one representative snapshot in Figure 2c). Because of the peroxide rotational motion around Fe−O_a (discussed above), these configurations take place when H_a is not buried beneath Phe41 but exposed to the water access channel (i.e., $-40 < \Omega < 120°$; see Figure S5, SI). Among all hydrated configurations, those in which a water molecule bridges H_a of the peroxide and N_ε of His42 are especially interesting as they could initiate catalysis via the wet mechanism (Figure 1b).[8] Such configurations, named "reactive conformations", occurred in 52 of the 4000 frames analyzed (1.3%). Analysis of each configuration reveals that the identity of the water molecule bridging the peroxide and the His42 (the catalytic water) might differ among reactive configurations (four different molecules were observed in the time frame analyzed; see Figure S3, SI), highlighting the mobility of the water molecules in the channel.

Channel Water Occupancy. To gain insight into the occupation of the heme access channel and distal side pocket by water molecules, we have mapped their position along the MD trajectory. Though most likely not converged within the time spanned by the simulation (4 ns excluding equilibration), the occupancy of the channel[62] displays a recognizable pattern (see Figure S6, SI), and preferred sites of interactions can be distinguished (Table S2, SI). These include the peroxide, the distal Arg, and the backbone carbonyl of Pro139 (Figure 2c). The different spots on the scatter plot in Figure S6 (SI) correspond to interplay between the total number of water molecules in the channel and distal pocket and the orientation

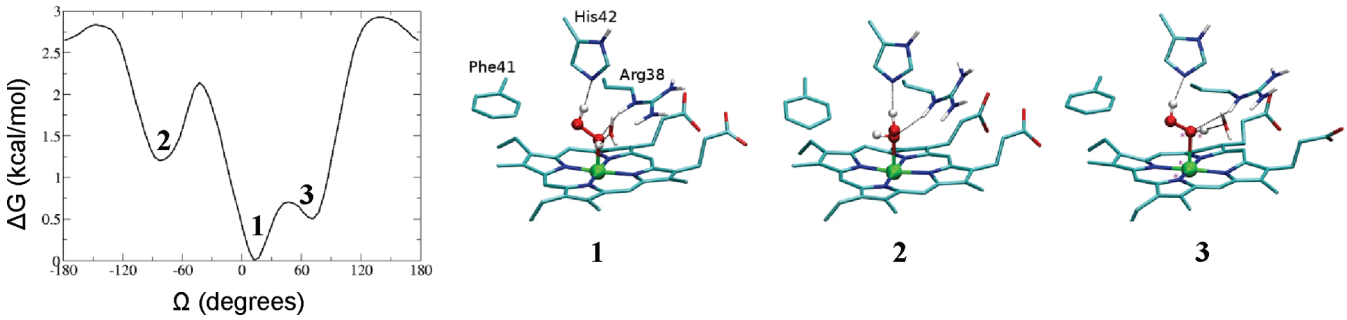

Figure 3. Free-energy profile for the rotation around the Fe−O_a bond (the collective variable used was the N_β−Fe−O_a−H_a dihedral, Ω). Selected snapshots corresponding to the most stable minima are shown. See Figure 1 for atom names.

of the above residues. Therefore, the results of the classical MD simulations show that (i) the channel is always hydrated, (ii) there are preferred sites of interaction for the water molecules in the channel, and (iii) the reactive conformation is reached within the nanosecond time scale.

3.2. Metadynamics Simulation: Rotation of H_2O_2 Around Fe−O. As discussed above, the H_2O_2 molecule rotates around the Fe−O_a bond, displaying three preferred orientations. Hydrated configurations, from which the reactive ones take place, are observed only for particular rotational orientations, that is, when H_a is exposed to the water access channel. We thus investigated the conformational freedom of hydrogen peroxide around the Fe−O_a bond by metadynamics. The resulting free-energy profile is shown in Figure 3. Three minima were observed at Ω = −80.0, 12.5, and 72.5°, in fair correspondence with the values of the most populated conformations observed in the equilibrium MD simulation (see above). The absolute minimum (Ω = 12.5°, **1** in Figure 3) corresponds to conformations in which H_a is oriented toward the main channel and is separated by a barrier of ∼2 kcal/mol from the conformations in which H_a is not water-exposed (buried beneath Phe41) (Ω = −80°, **2** in Figure 3), which lies 1.2 kcal/mol higher in energy. Although determined by many interactions, the energy difference between these two states may be interpreted as due to the extra H-bond that the peroxide may form when H_a is oriented toward the distal cavity. In the third minimum (Ω = 72.5°, **3** in Figure 3), H_a is also water-exposed. Analysis of distal side waters dynamics shows that the water−peroxide interactions are as observed in the equilibrium MD simulation. Therefore, hydrated configurations correspond to the most stable rotational conformations of H_2O_2.

3.3. Metadynamics Simulation: Water Motion in the Heme Access Channel. This simulation was performed to obtain the free-energy landscape of water motion in the access channel. The two collective variables used in the simulation (see the Computation Details section) describe the approach of one water molecule to the bound H_2O_2 (CV_1) and the proximity of this water molecule to the N_ε of the distal His (CV_2), respectively. Using these variables, we obtained the free-energy cost of reaching the reactive conformation. Furthermore, the simulation provided a picture of the most stable interaction sites of water along the channel and the energy barriers for translocation across these sites. The details of the metadynamics simulation (time evolution of the collective variables, selected distances/angles, rmsd, and free-energy surface) are given in the SI, Figures S7−S9.

The final free-energy surface (FES), obtained after several forward/backward reaction cycles of the metadynamics simulation, is shown in Figure 4. There are four minima (**B1**−**B4**) with similar stability (the maximum energy difference between

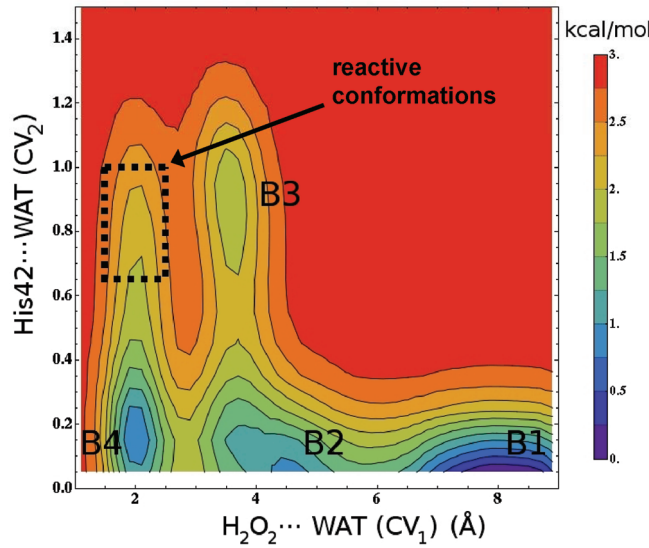

Figure 4. Free-energy landscape reconstructed after 5.5 ns of metadynamics simulation using the H_a···O^w distance (CV_1) and the N_ε of His42 ↔ H_1^w,H_2^w coordination number (CV_2) as collective variables. Energies are in kcal/mol. Isolines are spaced by 0.25 kcal/mol. The dashed box indicates the region corresponding to the reactive conformation defined in Figure 1b. See Figure 1 for atom names.

B1 and **B3** is just 2 kcal/mol), separated by small energy barriers (less than 1.5 kcal/mol). Figure 5 shows the structure of the heme pocket for a representative snapshot corresponding to each well of the FES (average geometrical parameters are given in Table S3, SI).

The most stable minimum (**B1**) corresponds to the reference water molecule being in the vestibule of the access channel (Figure 5), at ∼8 Å from the peroxide (CV_1 value in Figure 4). In this configuration, the water molecule forms several hydrogen bonds with other molecules of the channel (see the blue channel in Figure 2b). As the reference water molecule enters the channel, it reaches **B2**. This energy well captures at least two types of configurations. In the majority type, the water molecule interacts with Pro139 but is still far from His42 (∼5 Å, see Table S3 (SI), corresponding to a small CV_2 value in Figure 4). A less populated minority conformation is also observed, in which the reference water interacts with Arg38 (Figure S10, SI).

The water molecule may exit basin **B2** by either overcoming a barrier of 1.25 kcal/mol and entering basin **B3**, or passing a 1 kcal/mol barrier, entering basin **B4** (Figure 4). Interestingly, **B3** configurations are characterized by having a wire of two water molecules bridging H_a and the N_ε of the distal His (Figure 5). Because of the well-known ability of protons to translocate along water wires,[63] these configurations could facilitate proton

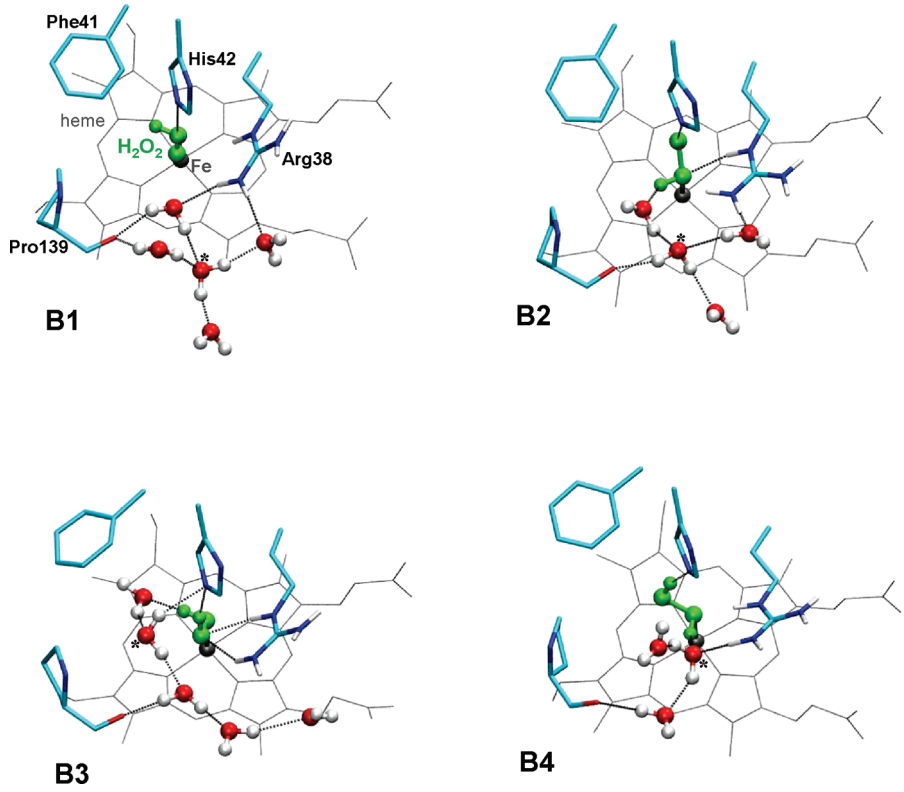

Figure 5. Selected snapshots named according to the basin on the FES to which they belong (Figure 4). The water molecule used in the definition of the collective variables is marked with an asterisk. The side chains of Arg38, Phe41, His42, and Pro139 and the heme group and water molecules hydrogen bonded to the reference water are shown. Only polar hydrogens are displayed.

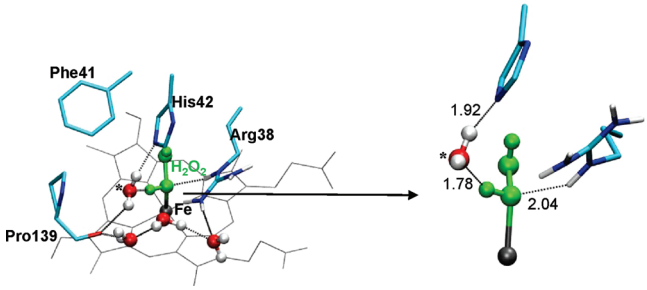

Figure 6. Representative snapshot corresponding to the reactive conformation (dashed box in Figure 4).

transfer from H_2O_2 to His, forming compound 0. This possibility has been investigated by QM/MM calculations, as described below.

B4 is characterized by a short distance between the reference water and H_2O_2. Here, the oxygen atom of the water molecule forms a hydrogen bond with H_a of H_2O_2 (see Figure 5), with an average $H_a\cdots O^w$ distance of 2.03 Å (Table S2, SI). Reactive configurations, in which the water molecule also interacts with the N_ε of His42 (Figure 6), appear as a shoulder of **B4** (region marked with a dashed box in Figure 4) lying only 1.25 kcal/mol above the local minimum. Therefore, configurations that could trigger catalysis via the wet mechanism (Figure 1b) are easily accessible. This is consistent with the occurrence of such conformations in an equilibrium MD simulation (section 3.1).

3.4. QM/MM Calculations. Once the water molecule reaches the reactive conformation, hydrogen peroxide can be easily deprotonated via the wet mechanism (Figure 1b) to form the $Fe^{III}-OOH$ species (Cpd 0). QM/MM calculations at the B3LYP/TZVP level (Figure S12, SI) show that the energy barrier for this process is 5.26 kcal/mol. Similar calculations starting from a configuration with two water molecules bridging H_2O_2 and His42 (i.e., conformations belonging to basin **B3**) show that such proton transfer is also feasible. The corresponding energy barrier, albeit larger (11.40 kcal/mol; Figure S13, SI) than that for the one-water mechanism, is still smaller than the one computed for the dry mechanism (21.5 kcal/mol).[8,26]

4. Discussion

A current issue in enzyme catalysis is the role played by individual water molecules; water molecules may shuttle protons, bridge long distances between reactants and catalytic residues, participate in proton-coupled electron transfer mechanisms, and so on.[63] Therefore, particular attention is directed to the elucidation of the potential role played by water in various enzymatic mechanisms.[64,65]

In this work, we have analyzed the dynamics of water molecules in the heme pocket of HRP and its implications for the mechanism of Cpd I formation. Our 4 ns long equilibrium MD simulations show that the active site of HRP is hydrated, with an average of 2.6 ± 1.1 water molecules within 5 Å from H_2O_2. Preferred interaction sites for H_2O include the peroxide, the distal Arg, and the backbone carbonyl of Pro139. Reactive conformations, as defined by those in which one water molecule bridges the peroxide and the distal His, occur with a probability of 1.3%. These results were further confirmed by metadynamics (MetD) simulations of water motion in the access channel of the heme. The reconstructed free-energy surface (Figure 4) shows that there are several preferred configurations, all accessible in terms of energy, for water molecules along the heme access channel. However, our MD and MetD simulation constitute a fairly rigorous method that leaves little doubt that water is present in the pocket. We do not understand at present the reason why the MD simulations of Zazza et al.[30,31] did not show any water molecule in the vicinity of hydrogen peroxide.

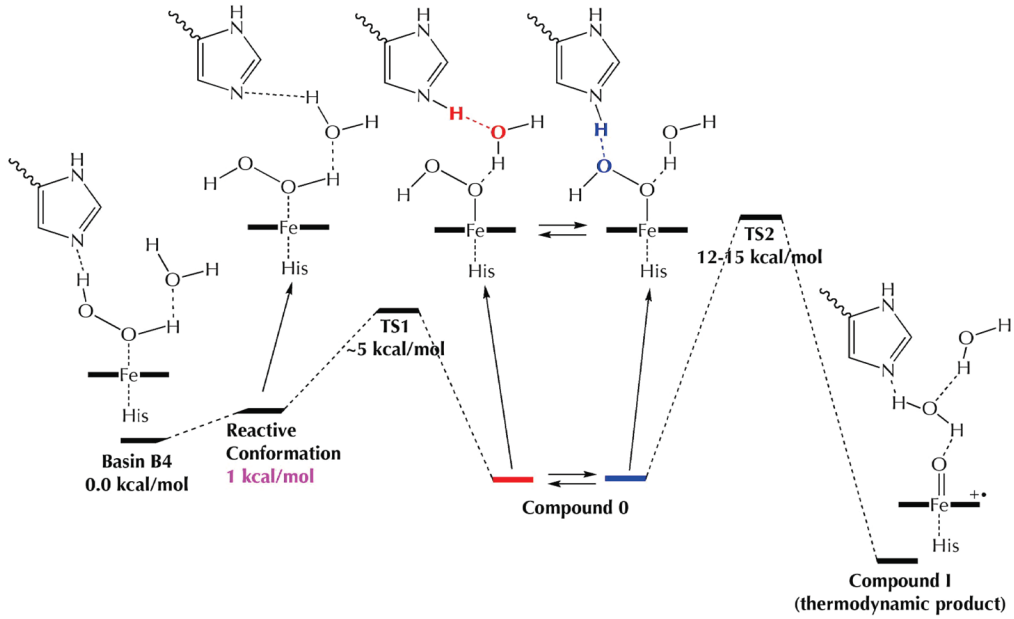

Figure 7. Proposed reaction mechanism of Cpd I formation in HRP.

This finding was attributed to Arg38 preventing the access of water molecules to Fe−H_2O_2, something that we did not observe in our calculations. The origin of the disparity is not well understood. It could be argued that it is due to technical differences among the two studies, such as the initial structures on which simulations were based (PDB codes: 1HCH, 1.57 Å resolution, in the present study and 1ATJ, 2.15 Å resolution, in refs 30 and 31) and the force field employed for the protein (AMBER versus gromos96), water (TIP3P versus SPC), and the Fe−H_2O_2 moiety. However, we think that it is unlikely that the use of a different force field leads to such opposite results. Therefore, we can only speculate that the protein could have been trapped in a dry state during the initial equilibration of the system. In our simulations, this problem, if present, would have been overcome by the use of metadynamics, which helps the system to escape from free-energy minima.[32] Overall, the finding that the channel is hydrated is in line with various experimental data; (a) the X-ray structures of most species in the HRP cycle were shown to include water molecules,[4] (b) water was shown to catalyze the formation of Cpd I in organic solvents,[13] and (c) use of labeled water shows incorporation of the label in H_2O_2.[24,66]

On the basis of the configurations from the MetD study in which water molecules bridge the peroxide and the distal His, QM/MM calculations show that the barrier for deprotonation is drastically reduced from 21.5 kcal/mol for the direct abstraction[8,26] to 5.3 kcal/mol for a single intervening water molecule (Figure S12, SI). However, when the bridge is constituted by two water molecules, the barrier reduction is not so effective (11.4 kcal/mol; see Figure S13, SI). The involvement of water as a means of lowering the barrier for proton-transfer reactions is an interesting feature emerging from recent theoretical studies of enzymatic systems. Siegbahn[27] suggested that a water molecule enters the Fe_2 binding site of class I ribonucleotide reductase and facilitates the transfer of a proton from Tyr122 to Asp84 during tyrosyl radical formation in subunit R2. De Vivo et al.[28,29] observed during CPMD simulations of epoxide hydrolase a water molecule intruding between Mg^{2+} and the substrate and mediating proton shuttle. Wang et al.[67] found a water-mediated mechanism in DNA polymerase IV from *Sulfolobus solfataricus*, in which bridging crystal water molecules relay successive proton-transfer events. A recent paper by Wang et al.[9] showed the intriguing role of water molecules in inducing catalysis of a distant substrate by a P450 enzyme. Metadynamics simulations by Boero et al. demonstrated that one solvent water acts as a trigger in the initial phase of the adenosine triphosphate (ATP) hydrolysis in ATP synthase.[68] Our modeling expands the case studies in which individual water molecules are found to facilitate proton-transfer events and furthermore suggests that water molecules may act as catalysts not only from stable, bound conformations but also in transient conformations. This behavior appears to be fundamental in the present case because in the second step of the process, that is, from Cpd 0 to Cpd I, the back proton transfer from His42 to O_b (Figure 1) does not need the presence of the water molecule that facilitated the first proton transfer from O_a to His42. Thus, to act effectively, a water molecule should easily reach the reactive conformation (Figure 1b, left) without being tightly bound in order to be able to "step aside" and let the reaction proceed further to the next step. The free-energy surface computed by metadynamics simulation show the reactive conformation lying on a shoulder 1 kcal/mol above the local minimum, exactly the type of landscape that we would expect to achieve the above behavior.

The overall mechanism of Cpd I formation that arises from our calculations, shown in Figure 7, is essentially the Poulos−Kraut one, but it differs from it in the first step of the process, that is, formation of Cpd 0, in that a water molecule assists the proton transfer from O_a to His42. According to our computed mechanism, the rate-limiting step of the process is the step from Cpd 0 to Cpd I, which consists of O−O breakage and concomitant protonation of the leaving oxygen to form a water molecule. As noted above, a recent isotopic labeling study showed that HRP turnover conducted from nonlabeled hydrogen peroxide and isotopically labeled water results in the isotopic enrichment of the hydrogen peroxide.[24] This finding led the authors to conclude that formation of Cpd I is reversible and that the O−O breaking is not the rate-limiting step.[24] Concerning the possibility of the process being reversible, the high barrier (12−15 kcal/mol) and high exothermicity of the reaction (~30 kcal/mol) as displayed by the energy profile in Figure 7 (see also Figure S13) indicate that the reverse process is characterized

by a sizable barrier. Similar energy barriers have been observed so far for Cpd I formation in a variety of heme enzymes such as P450,[69,70] CPO,[71,72] and NOS.[73] Our computed barrier (12−15 kcal/mol), though not including zero-point energy (estimated to decrease the computed barrier by ∼3 kcal/mol) and tunneling effects (which are not dramatic according to kinetic studies), is in agreement with the one derived from kinetics.[14] Nevertheless, the mass-law effect of water (55.6M) may, as suggested by Rietjens et al,[66] render the reverse reaction fast enough to be detected on the time scale of the isotopic experiment. Alternatively, it might be that incorporation of ^{18}O via water molecules occurs before formation of Cpd I (e.g., preexchange by nucleophilic cleavage of H_2O_2). The calculations presented in this work point to the close interactions between water molecules and peroxide in both the $Fe^{III}-H_2O_2$ complex and Cpd 0. These interactions may be the key toward an understanding of the results of isotopic labeling experiments, and calculations are on the way in our lab to investigate this hypothesis. Therefore, at present, a definitive theoretical explanation for the $^{18}O/^{16}O$ scrambling observed experimentally is still elusive. Be this as it may, the scrambling clearly supports the presence of water in the enzyme throughout the catalytic cycle, and hence, it favors our one-water mechanism (Figure 1b) over a dry mechanism. Concerning the possibility of the O−O cleavage not being the rate-limiting step of the process, the study of Roth and Cramer,[24] as well as ours,[8] does not reveal any intermediate after the O−O breaking step, which makes this interpretation questionable.

In summary, our calculations provide a route to Cpd I in which water plays an active role in the initial acid−base step of the reaction. Therefore, we conclude that (i) Cpd 0 formation in HRP follows the wet mechanism and (ii) the subsequent protonation of the distal peroxide oxygen by His42 with the concomitant breakage of the OO bond is the rate-limiting step of the process.

Our previous[8] and present studies on the subject, taken together, highlight an effective procedure to investigate chemical reactions which are of local nature (e.g., bond breakage/formation), classical molecular dynamics and free-energy calculations to characterize the conformational space of the system of interest and static QM/MM potential energy scans on selected conformations to determine the energy barrier for the chemical transformation. The strength of the outlined procedure lies in the affordable computational cost of static calculations subject to the requirement of ascertaining that the starting conformation does not lay too high on the free-energy landscape.

Acknowledgment. The authors thank the Israel Science Foundation (ISF Grant 16/06 to S.S.), the Spanish Ministry of Science and Innovation (MICINN) (Grant FIS2008-03845), the Generalitat de Catalunya (Grant 2009SGR-1309), and the CRIHAN (Project 2006013) for its financial assistance. P.V. acknowledges an Juan de la Cierva contract from MCINN. We acknowledge the computer support, technical expertise, and assistance provided by the Barcelona Supercomputing Center-Centro Nacional de Supercomputación (BSC-CNS).

Supporting Information Available: Parameters used in the classical simulations (MD and MetD), selected snapshots, evolution of selected structural parameters, and water occupancy along the access channel. Reaction QM/MM energies for Cpd I formation at the B3LYP/TZVP level. This material is available free of charge via the Internet at http://pubs.acs.org.

References and Notes

(1) Messerschmidt, A.; Cygler, M.; Bode, W. *Handbook of metalloproteins*; Wiley: Chichester, U.K., 2001.
(2) Dunford, H. B. *Heme peroxidases*; John Wiley: New York; Chichester, U.K., 1999.
(3) Poulos, T. L. *Nat. Prod. Rep.* **2007**, *24*, 504–510.
(4) Berglund, G. I.; Carlsson, G. H.; Smith, A. T.; Szoke, H.; Henriksen, A.; Hajdu, J. *Nature.* **2002**, *417*, 463–468.
(5) Santos, R.; Hritz, J.; Oostenbrink, C. *J. Chem. Inf. Model.* **2010**, *50*, 146−154.
(6) Scorciapino, M. A.; Robertazzi, A.; Casu, M.; Ruggerone, P.; Ceccarelli, M. *J. Am. Chem. Soc.* **2010**, doi: 10.1021/ja909822d.
(7) Jones, P.; Dunford, H. B. *J. Inorg. Biochem.* **2005**, *99*, 2292–2298.
(8) Derat, E.; Shaik, S.; Rovira, C.; Vidossich, P.; Alfonso-Prieto, M. *J. Am. Chem. Soc.* **2007**, *129*, 6346–6347.
(9) Wang, Y.; Chen, H.; Makino, M.; Shiro, Y.; Nagano, S.; Asamizu, S.; Onaka, H.; Shaik, S. *J. Am. Chem. Soc.* **2009**, *131*, 6748–6762.
(10) Cho, K. B.; Derat, E.; Shaik, S. *J. Am. Chem. Soc.* **2007**, *129*, 3182–3188.
(11) Baek, H. K.; Van Wart, H. E. *Biochemistry.* **1989**, *28*, 5714–5719.
(12) Baek, H. K.; Van Wart, H. E. *J. Am. Chem. Soc.* **1992**, *114*, 718–725.
(13) Ozaki, S.; Inada, Y.; Watanabe, Y. *J. Am. Chem. Soc.* **1998**, *120*, 8020–8025.
(14) Hiner, A. N.; Raven, E. L.; Thorneley, R. N.; Garcia-Canovas, F.; Rodriguez-Lopez, J. N. *J. Inorg. Biochem.* **2002**, *91*, 27–34.
(15) Jones, P.; Dunford, H. B. *J. Theor. Biol.* **1977**, *69*, 457–470.
(16) Poulos, T. L.; Freer, S. T.; Alden, R. A.; Edwards, S. L.; Skogland, U.; Takio, K.; Eriksson, B.; Xuong, N.; Yonetani, T.; Kraut, J. *J. Biol. Chem.* **1980**, *255*, 575–580.
(17) Poulos, T. L.; Kraut, J. *J. Biol. Chem.* **1980**, *255*, 8199–8205.
(18) Rodriguez-Lopez, J. N.; Smith, A. T.; Thorneley, R. N. *J. Biol. Chem.* **1996**, *271*, 4023–4030.
(19) Erman, J. E.; Vitello, L. B.; Miller, M. A.; Shaw, A.; Brown, K. A.; Kraut, J. *Biochemistry.* **1993**, *32*, 9798–9806.
(20) Vitello, L. B.; Erman, J. E.; Miller, M. A.; Wang, J.; Kraut, J. *Biochemistry.* **1993**, *32*, 9807–9818.
(21) Kuhnel, K.; Derat, E.; Terner, J.; Shaik, S.; Schlichting, I. *Proc. Natl. Acad. Sci. U.S.A.* **2007**, *104*, 99–104.
(22) Unno, M.; Chen, H.; Kusama, S.; Shaik, S.; Ikeda-Saito, M. *J. Am. Chem. Soc.* **2007**, *129*, 13394–13395.
(23) Dunford, H. B.; Hewson, W. D.; Steiner, H. *Can. J. Chem.* **1978**, *56*, 2844–2852.
(24) Roth, J. P.; Cramer, C. J. *J. Am. Chem. Soc.* **2008**, *130*, 7802–7803.
(25) Miller, M. A.; Shaw, A.; Kraut, J. *Nat. Struct. Biol.* **1994**, *1*, 524–531.
(26) Derat, E.; Shaik, S. *J. Phys. Chem. B.* **2006**, *110*, 10526–10533.
(27) Siegbahn, P. E. M. *Q. Rev. Biophys.* **2003**, *36*, 91–145.
(28) De Vivo, M.; Ensing, B.; Dal Peraro, M.; Gomez, G. A.; Christianson, D. W.; Klein, M. L. *J. Am. Chem. Soc.* **2007**, *129*, 387–394.
(29) De Vivo, M.; Ensing, B.; Klein, M. L. *J. Am. Chem. Soc.* **2005**, *127*, 11226–11227.
(30) Zazza, C.; Amadei, A.; Palma, A.; Sanna, N.; Tatoli, S.; Aschi, M. *J. Phys. Chem. B.* **2008**, *112*, 3184–3192.
(31) Tatoli, S.; Zazza, C.; Sanna, N.; Palma, A.; Aschi, M. *Biophys. Chem.* **2009**, *141*, 87–93.
(32) Laio, A.; Parrinello, M. *Proc. Natl. Acad. Sci. U.S.A.* **2002**, *99*, 12562–12566.
(33) Collins, J. R.; Du, P.; Loew, G. H. *Biochemistry* **1992**, *31*, 11166–11174.
(34) De Gioia, L.; Fantucci, P. *J. Mol. Struct.: THEOCHEM* **1999**, *469*, 41–53.
(35) Filizola, M.; Loew, G. H. *J. Am. Chem. Soc.* **2000**, *122*, 3599–3605.
(36) Cornell, W. D.; Cieplak, P.; Bayly, C. I.; Gould, I. R.; Merz, K. M.; Ferguson, D. M.; Spellmeyer, D. C.; Fox, T.; Caldwell, J. W.; Kollman, P. A. *J. Am. Chem. Soc.* **1995**, *117*, 5179–5197.
(37) Cheatham, T. E.; Cieplak, P.; Kollman, P. A. *J. Biomol. Struct. Dyn.* **1999**, *16*, 845–862.
(38) Jorgensen, W. L.; Chandrasekhar, J.; Madura, J. D.; Impey, R. W.; Klein, M. L. *J. Chem. Phys.* **1983**, *79*, 926–935.
(39) Wang, J. M.; Wolf, R. M.; Caldwell, J. W.; Kollman, P. A.; Case, D. A. *J. Comput. Chem.* **2004**, *25*, 1157–1174.
(40) Bayly, C. I.; Cieplak, P.; Cornell, W. D.; Kollman, P. A. *J. Phys. Chem.* **1993**, *97*, 10269–10280.
(41) Car, R.; Parrinello, M. *Phys. Rev. Lett.* **1985**, *55*, 2471–2474.
(42) Hohenberg, P.; Kohn, W. *Phys. Rev. B.* **1964**, *136*, B864.
(43) Kohn, W.; Sham, L. J. *Phys. Rev.* **1965**, *140*, 1133.
(44) Troullier, N.; Martins, J. L. *Phys. Rev. B* **1991**, *43*, 1993–2006.
(45) Becke, A. D. *J. Chem. Phys.* **1986**, *84*, 4524–4529.
(46) Perdew, J. P. *Phys. Rev. B* **1986**, *33*, 8822–8824.

(47) Martyna, G. J.; Tuckerman, M. E. *J. Chem. Phys.* **1999**, *110*, 2810–2821.
(48) Hoover, W. G. *Phys. Rev. A* **1985**, *31*, 1695–1697.
(49) Nose, S. *Mol. Phys.* **1984**, *52*, 255–268.
(50) Phillips, J. C.; Braun, R.; Wang, W.; Gumbart, J.; Tajkhorshid, E.; Villa, E.; Chipot, C.; Skeel, R. D.; Kale, L.; Schulten, K. *J. Comput. Chem.* **2005**, *26*, 1781–1802.
(51) Iannuzzi, M.; Laio, A.; Parrinello, M. *Phys. Rev. Lett.* **2003**, *90*, 238302.
(52) Sherwood, P.; de Vries, A. H.; Guest, M. F.; Schreckenbach, G.; Catlow, C. R. A.; French, S. A.; Sokol, A. A.; Bromley, S. T.; Thiel, W.; Turner, A. J.; Billeter, S.; Terstegen, F.; Thiel, S.; Kendrick, J.; Rogers, S. C.; Casci, J.; Watson, M.; King, F.; Karlsen, E.; Sjovoll, M.; Fahmi, A.; Schafer, A.; Lennartz, C. *J. Mol. Struct.: THEOCHEM* **2003**, *632*, 1–28.
(53) Ahlrichs, R.; Bar, M.; Haser, M.; Horn, H.; Kolmel, C. *Chem. Phys. Lett.* **1989**, *162*, 165–169.
(54) Smith, W.; Forester, T. R. *J. Mol. Graph.* **1996**, *14*, 136–141.
(55) Becke, A. D. *Phys. Rev. A* **1988**, *38*, 3098–3100.
(56) Becke, A. D. *J. Chem. Phys.* **1993**, *98*, 5648–5652.
(57) Lee, C.; Yang, W.; Parr, R. *Phys. Rev. B* **1988**, *37*, 785–789.
(58) Friesner, R. A.; Murphy, R. B.; Beachy, M. D.; Ringnalda, M. N.; Pollard, W. T.; Dunietz, B. D.; Cao, Y. X. *J. Phys. Chem. A* **1999**, *103*, 1913–1928.
(59) Hay, P. J.; Wadt, W. R. *J. Chem. Phys.* **1985**, *82*, 299–310.
(60) Schafer, A.; Huber, C.; Ahlrichs, R. *J. Chem. Phys.* **1994**, *100*, 5829–5835.
(61) MacKerell, A. D.; Bashford, D.; Bellott, M.; Dunbrack, R. L.; Evanseck, J. D.; Field, M. J.; Fischer, S.; Gao, J.; Guo, H.; Ha, S.; Joseph-McCarthy, D.; Kuchnir, L.; Kuczera, K.; Lau, F. T. K.; Mattos, C.; Michnick, S.; Ngo, T.; Nguyen, D. T.; Prodhom, B.; Reiher, W. E.; Roux, B.; Schlenkrich, M.; Smith, J. C.; Stote, R.; Straub, J.; Watanabe, M.; Wiorkiewicz-Kuczera, J.; Yin, D.; Karplus, M. *J. Phys. Chem. B* **1998**, *102*, 3586–3616.
(62) Rydberg, P.; Rod, T. H.; Olsen, L.; Ryde, U. *J. Phys. Chem. B* **2007**, *111*, 5445–5457.
(63) Ball, P. *Chem. Rev.* **2008**, *108*, 74–108.
(64) Makris, T. M.; von Koenig, K.; Schlichting, I.; Sligar, S. G. *Biochemistry* **2007**, *46*, 14129–14140.
(65) Matsui, T.; Furukawa, M.; Unno, M.; Tomita, T.; Ikeda-Saito, M. *J. Biol. Chem.* **2005**, *280*, 2981–2989.
(66) van Haandel, M. J. H.; Primus, J. L.; Teunis, C.; Boersma, M. G.; Osman, A. M.; Veeger, C.; Rietjens, I. *Inorg. Chim. Acta* **1998**, *276*, 98–105.
(67) Wang, L. H.; Yu, X. Y.; Hu, P.; Broyde, S.; Zhang, Y. K. *J. Am. Chem. Soc.* **2007**, *129*, 4731–4737.
(68) Boero, M.; Ikeda, T.; Ito, E.; Terakura, K. *J. Am. Chem. Soc.* **2006**, *128*, 16798–16807.
(69) Altun, A.; Shaik, S.; Thiel, W. *J. Comput. Chem.* **2006**, *27*, 1324–1337.
(70) Shaik, S.; Cohen, S.; Wang, Y.; Chen, H.; Kumar, D.; Thiel, W. *Chem. Rev.* **2010**, *110*, 949.
(71) Chen, H.; Hirao, H.; Derat, E.; Schlichting, I.; Shaik, S. *J. Phys. Chem. B* **2008**, *112*, 9490–9500.
(72) Lai, W.; Chen, H.; Shaik, S. *J. Phys. Chem. B* **2009**, *113*, 7912–7917.
(73) Cho, K. B.; Carvajal, M. A.; Shaik, S. *J. Phys. Chem. B* **2009**, *113*, 336–346.

JP911170B